

# Towards a Foothold Evaluation Criterion for Dynamic Transition Feasibility

Angelo Bratta<sup>1</sup>, Luca Clemente<sup>1,2</sup>, Octavio Villarreal<sup>1</sup>, Michele Focchi<sup>1</sup>, Victor Barasuol<sup>1</sup>,  
Giovanni Gerardo Muscolo<sup>3</sup>, and Claudio Semini<sup>1</sup>

**Abstract**—In this extended abstract we give a brief introduction to our work [1]. We propose a foothold evaluation criterion that considers the transition feasibility for both linear and angular dynamics to overcome complex scenarios. We present convex and nonlinear formulations as a direct extension of [2] in a receding-horizon fashion to take into account also angular dynamics. The criterion is integrated with a Vision-based Foothold Adaptation (VFA) strategy that considers robot kinematics, leg collisions and terrain morphology. We verify the validity of the selected footholds and of the generated trajectories in simulation and experiments with the 90kg quadruped robot HyQ.

*Paper type – Recent Work [1]*

## I. INTRODUCTION

Optimization-based techniques allow legged robots to react, adapt and navigate in complex scenarios, choosing a trajectory for the motion of its base, and decide a feasible contact sequence for its feet to follow the base. Motions and contacts need to be both dynamically (e.g., inside the torque limits of the robot’s actuators or not falling) and kinematically feasible (e.g., inside the joints’ range of motion).

We categorize two main ways to tackle the problem: (a) coupled approaches, in which the base trajectory and footholds are optimized jointly, and (b) decoupled approaches, in which the footholds are selected first and then the trajectory is optimized to follow the footholds.

Coupled approaches find a reference (position and orientation) for the body, contact locations (footholds), and inputs (ground reaction forces (GRFs), torques), for a defined planning horizon. The main advantage of coupled approaches is that we can guarantee that the trajectories are realizable by the robot, enforcing kinematic and dynamic constraints in the formulation. In particular, [3] uses the single rigid body dynamics model (SRBDM) to make the nonlinear program treatable, [4] solves the optimization problem via sequential linear quadratic and [5] computes gait pattern, contact sequence, and center of mass (CoM) trajectories as an outcome of a mixed-integer convex programs. However, all of these suffer from large computational times and risk getting stuck in local minima.

Decoupled approaches, instead, outsource the foothold selection to an external module. This relieves computational

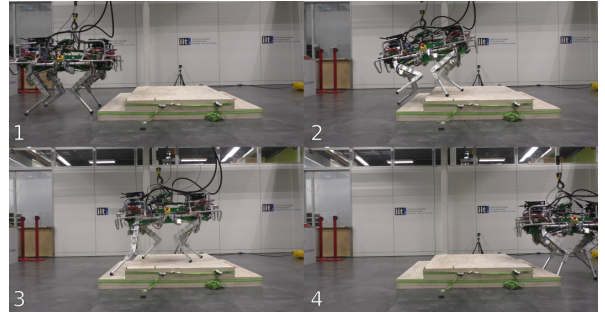


**Fig. 1:** Snapshots of the HyQ robot climbing stair scenario using the proposed foothold evaluation criterion for dynamic transition feasibility.

effort from the optimization, since the foothold positions have a nonlinear relationship with the CoM position [6]. Kalakrishnan et al. [7] discretized the problem by considering templates corresponding to portions of the map in the vicinity of a nominal landing position. Inspired by this, methods have resorted to template-based foothold selection using learning-based [8], [9], [10], [11], [12], [13] or fast optimization [14], [15] strategies. The main drawback is that there is no guarantee that given the selected footholds a dynamically feasible trajectory for the CoM exists. Fernbach et al. [2] presented a method to evaluate the transition feasibility of a motion with contact switches. The method relies on the parameterization of the trajectory of the CoM as a Bézier curve, which allows to pose the problem as a quadratic program. The method here presented is based on [2].

Our main contributions are:

- 1) A dynamic transition feasibility foothold evaluation that considers linear and angular dynamics of the SRBDM. We implemented in simulation and experiments two formulations that consider CoM motion and base orientation; a convex one (based on [2]) that includes angular dynamics without breaking convexity and a novel nonlinear approach.
- 2) A comparison between a convex and a nonlinear formulation for different scenarios in terms of quality of the generated trajectories.

In this extended abstract we mainly expose the first point.

## II. CONTACT TRANSITION FEASIBILITY WITH ANGULAR DYNAMICS

Starting from [2], we include angular quantities to the set of states. Thus, a state is defined as  $\mathbf{x}(t) = [\mathbf{c}(t) \dot{\mathbf{c}}(t) \ddot{\mathbf{c}}(t) \Theta(t) \dot{\Theta}(t) \ddot{\Theta}(t)]^T \in \mathbb{R}^{6 \times 3}$ , where  $\mathbf{c}$  is the position of the CoM and  $\Theta$  is the orientation of the

<sup>1</sup> Dynamic Legged Systems (DLS) lab, Istituto Italiano di Tecnologia (IIT), Genova (Italy). *firstname.lastname@iit.it*.

<sup>2</sup> Department of Electronics and Telecommunications, Collegio di Ingegneria Informatica, del Cinema e Meccatronica, Politecnico di Torino, Turin (Italy).

<sup>3</sup>Department of Computer Science, University of Verona, Verona (Italy).

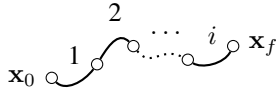


**Fig. 2:** Example of sub-horizon partitioning. The CoM trajectory connecting the initial ( $\mathbf{x}_0$ ) and the final ( $\mathbf{x}_f$ ) states is partitioned into multiple sub-horizons. Each of them is labeled according to an increasing index  $i$  and is subject to a different set of constraints.

base, expressed in terms of roll ( $\phi$ ), pitch ( $\gamma$ ) and yaw ( $\psi$ ) angles.

A feasible dynamic transition subject to dynamics constraints that connects two sets of states is defined as  $\mathbf{f}(t) : \mathbf{x}(t_0) \rightarrow \mathbf{x}(t_f)$ ,  $t_f > t_0$ , where  $t_0$  and  $t_f$  correspond to the initial and final states respectively. We employ continuously differentiable, parametric curves to describe position and orientation.

#### A. Time horizon description

We choose to express the considered time horizon in terms of *contact switches* to have a general description, applicable to any type of gait. A contact switch happens whenever any foot makes or breaks a contact with the ground. We define a contact switch horizon (CSH) as the number of non-simultaneous contact switches occurring in the considered period  $T = t_f - t_0$ .

We adopt a CSH partitioning method (*sub-horizon*, Fig. 2). We choose to limit each sub-horizon to two contact switches to prevent the reduction of the solution space. Such limit is specifically chosen to connect two sub-sequent stance phases, i.e., lift-off and touchdown of the same leg. Then, to evaluate an arbitrarily large CSH, we concatenate multiple sub-horizons by means of continuity constraints in the *way-points* (connection points between sub-curves).

We adopt the SRBDM to assert dynamic transition feasibility:

$$\underbrace{\begin{bmatrix} m(\ddot{\mathbf{c}} - \mathbf{g}) \\ m\mathbf{c} \times (\ddot{\mathbf{c}} - \mathbf{g}) + \dot{\mathbf{L}} \end{bmatrix}}_{\mathbf{w}} = \underbrace{\begin{bmatrix} \mathbf{I}_3 & \dots & \mathbf{I}_3 \\ [\mathbf{p}_1]_{\times} & \dots & [\mathbf{p}_j]_{\times} \end{bmatrix}}_{\mathbf{A}} \mathbf{f} \quad (1)$$

where  $\mathbf{g}$  is the gravity vector,  $\mathbf{I}_3 \in \mathbb{R}^{3 \times 3}$  is the identity matrix,  $\mathbf{f} = [\mathbf{f}_1 \dots \mathbf{f}_j]^T$ ,  $\mathbf{f}_j \in \mathbb{R}^3$  is the GRF associated to the  $j^{\text{th}}$  at point  $\mathbf{p}_j \in \mathbb{R}^3$  expressed in the world frame and  $m$  is the robot's mass. We express  $\dot{\mathbf{L}}$  as a function of the angular quantities (orientation, rate and acceleration) by analytically differentiating  $\mathbf{L} = \mathbf{I}_{\mathcal{W}}\boldsymbol{\omega}$ , where  $\boldsymbol{\omega}$  is angular velocity of the rigid body expressed in the CoM frame.

$$\dot{\mathbf{L}} = \underbrace{\mathbf{T}\dot{\boldsymbol{\Theta}} \times \mathbf{I}_{\mathcal{W}}\mathbf{T}\dot{\boldsymbol{\Theta}}}_{\dot{\mathbf{I}}_{\mathcal{W}}\boldsymbol{\omega}} + \underbrace{\mathbf{I}_{\mathcal{W}} \cdot (\dot{\mathbf{T}}\dot{\boldsymbol{\Theta}} + \mathbf{T}\ddot{\boldsymbol{\Theta}})}_{\mathbf{I}_{\mathcal{W}}\dot{\boldsymbol{\omega}}} \quad (2)$$

Note that (2) is a highly nonlinear expression that depends on  $\boldsymbol{\Theta}$  and its derivatives.

In the following sections we describe the two proposed formulations (*convex* and *nonlinear*) to solve the dynamic transition feasibility problem while accounting for the rate of change of angular momentum  $\dot{\mathbf{L}}$ . The first formulation aims at preserving the convexity of the problem, thus making

it less computationally demanding and not prone to local minima, at the cost of a more limited solution space. The second formulation offers a wider solution space with a larger computational cost.

#### B. Convex formulation

For each sub-horizon we parameterize the CoM trajectory with an  $8^{\text{th}}$  order Bézier curve to define the trajectory up to its third analytical derivative. Each sub-curve has a free control point. The collected points are used as optimization variables ( $\boldsymbol{\rho}$ ). To include the angular momentum rate  $\dot{\mathbf{L}}$  preserving convexity, we define  $\dot{\mathbf{L}}$  as an optimization variable and compute a desired  $\dot{\mathbf{L}}_{ref}$ , which is then tracked by including the term  $\|\dot{\mathbf{L}} - \dot{\mathbf{L}}_{ref}\|_2^2$  in the cost function. To compute  $\dot{\mathbf{L}}_{ref}$ , we define a desired angular behaviour of the robot by designing Bézier curves for the angular variables ( $\boldsymbol{\Theta}$ ,  $\dot{\boldsymbol{\Theta}}$ ,  $\ddot{\boldsymbol{\Theta}}$ ) and then computing the angular momentum rate with the full expression (2). We then formulate the optimization problem as:

$$\min_{\boldsymbol{\rho}, \dot{\mathbf{L}}} \sum_{k=0}^{N-i} \|\dot{\mathbf{L}}_k - \dot{\mathbf{L}}_{ref, k}\|_2^2 + \|\ddot{\mathbf{c}}_k(\boldsymbol{\rho}_i)\|_2^2$$

$$\text{subject to } \mathbf{w}_k(\boldsymbol{\rho}_i) = \mathbf{A}_k \mathbf{f}_k \quad (3a)$$

$$0 \leq f_{z, k} \leq f_{max} \quad (3b)$$

$$|f_{x, k}| \leq \mu f_{z, k}, \quad |f_{y, k}| \leq \mu f_{z, k} \quad (3c)$$

where  $f_{max}$  is an upper limit for the  $z$  direction of the force that the robot can exert on the ground. The tracking cost for the desired angular momentum rate is given by  $\|\dot{\mathbf{L}} - \dot{\mathbf{L}}_{ref}\|_2^2$  and we minimize the accelerations ( $\|\ddot{\mathbf{c}}(\boldsymbol{\rho})\|_2^2$ ) to incentivize smoother trajectories. This first method of including  $\dot{\mathbf{L}} \neq 0$  differs from [2] since we are not directly including  $\dot{\mathbf{L}}$  as a parametric curve, but rather expressing  $\dot{\mathbf{L}}$  as a function of a desired angular trajectory.

#### C. Nonlinear formulation

We present an alternative formulation to the one presented in Section II-B. The main difference is that herein we aim to directly optimize the trajectories of the angular quantities along the CSH, instead of using them as parameters to generate and track a desired  $\dot{\mathbf{L}}$ . The problem is nonlinear due to the dependency of  $\dot{\mathbf{L}}$  with respect to the angular position, velocity and acceleration. We then define a set of *enhanced states* as  $\bar{\mathbf{x}} = \mathbf{x}_d + \mathbf{x}_v$ , composed by a desired  $\mathbf{x}_d = [\mathbf{c}_d \ \dot{\mathbf{c}}_d \ \ddot{\mathbf{c}}_d \ \boldsymbol{\Theta}_d \ \dot{\boldsymbol{\Theta}}_d \ \ddot{\boldsymbol{\Theta}}_d]^T$  and a variable  $\mathbf{x}_v = [\Delta \mathbf{c} \ 0 \ \Delta \ddot{\mathbf{c}} \ 0 \ 0 \ 0]^T$  part, where  $\Delta \mathbf{c} \in \mathbb{R}^3$  and  $\Delta \ddot{\mathbf{c}}_v \in \mathbb{R}^3$  are decision variables.

We consider velocity and position/orientation variables as commanded quantities. Although they are not enhanced, they are still allowed to vary in between user-defined states in order to reach the designated value at each way-point while fulfilling the imposed constraints. The optimization problem

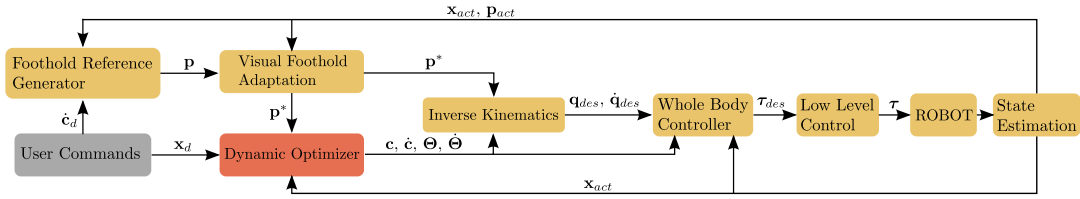


Fig. 3: Locomotion control pipeline used to implement the proposed foothold evaluation strategies in both experiments and simulations.

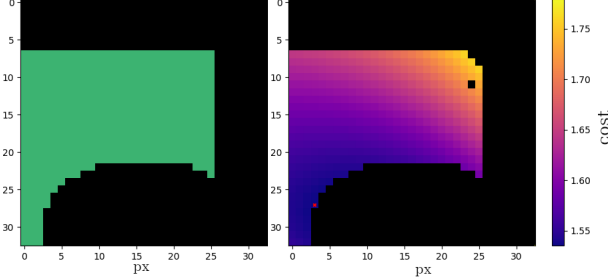


Fig. 4: Comparison of Vision-based Foothold Adaptation (VFA) (terrain roughness, kinematic reachability, collisions) versus dynamic foothold evaluation for the RF foot during stair climbing. In the case of the VFA evaluation, green pixels indicate safe landing locations and black unsafe. For the dynamic evaluation black pixels are dynamically infeasible footholds and we show the cost from the solution of (4a) indicated by the colorbar.

is then built as follows:

$$\min_{\rho, f, \Delta c, \Delta \dot{c}, \Theta, \dot{\Theta}, \ddot{\Theta}} \sum_{k=0}^{N \cdot i} \|\dot{\mathbf{L}}_k\|_2^2 + \|\ddot{\mathbf{c}}_k(\rho_i, \Delta \dot{\mathbf{c}}_i)\|_2^2 \quad (4a)$$

$$\text{subject to} \quad \mathbf{w}_k(\rho_i, \Delta \mathbf{c}_i, \Delta \dot{\mathbf{c}}_i) = \mathbf{A}_k \mathbf{f}_k \quad (4b)$$

$$\dot{\mathbf{L}}_k = \dot{\mathbf{L}}_f(\Theta_k, \dot{\Theta}_k, \ddot{\Theta}_k) \quad (4c)$$

$$\mathbf{X}_0 = \mathbf{X}_f \quad (4d)$$

$$0 \leq f_{z, k} \leq f_{max} \quad (4e)$$

$$|f_{x, k}| \leq \mu f_{z, k}, \quad |f_{y, k}| \leq \mu f_{z, k} \quad (4f)$$

where the cost function is similar to the one adopted in the convex formulation. The main difference consists in  $\|\dot{\mathbf{L}}_k\|_2^2$ , which is a cost term that aims at reducing the angular variation rather than tracking a reference behavior, helping to incentivize less aggressive motions for the angular quantities. We then consider (2) as a constraint dependent in the angular quantities defined as  $\dot{\mathbf{L}}_f(\Theta, \dot{\Theta}, \ddot{\Theta})$  and account for these quantities as decision variables.

This formulation is computationally more expensive than the convex formulation and it is prone to local minima, but the output trajectories present less peaks in acceleration compared to the convex formulation solutions. In addition, this method does not require to set extra constraints to maintain physical consistency.

### III. RESULTS

In this section we demonstrate the effectiveness of the proposed evaluation criterion for both formulations. We show an example of an evaluation of a series of contact locations for foothold selection and verify the feasibility of the generated trajectories in a stair climbing scenario. Additional results on flat terrain are reported in [1] and shown in the attached video <sup>1</sup>.

<sup>1</sup><https://www.youtube.com/watch?v=2rBopUquyrc>

#### A. Implementation details

To verify the feasibility of the generated trajectories provided by the foothold evaluation, we adopt the control scheme shown in Fig. 3. The Foothold Reference Generator is in charge of generating the foothold positions with respect to the actual CoM states and foothold positions  $(\mathbf{x}_{act}, \mathbf{p}_{act})$ , according to the user commanded velocity. The reference foothold positions are evaluated with the VFA [9], which discards unsuitable footholds according to geometric constraints around a nominal foothold, which is located at the centre of the heightmap. The footholds are adapted by selecting the safe foothold (according to the VFA) that is closest to the nominal one. The adapted footholds  $\mathbf{p}^* \in \mathbb{R}^{n_c \times 3}$  are sent to both the Dynamic Optimizer and IK blocks, for all the contact points  $nc$ . The Dynamic Optimizer block encapsulates the methods presented in this paper, which evaluate the dynamic feasibility of the foothold. If the adapted foothold is dynamically unfeasible, the feasibility of neighbouring footholds is assessed until a dynamically feasible one is found. Additional information on this procedure can be found in [1]. Regarding computation times, the convex formulation takes 2.90s for the stair scenario and 2.96s for the flat scenario in average over multiple trials to solve the optimization problem, whereas the nonlinear formulation takes 12.78s for the stair scenario and 8.0s for the flat scenario.

#### B. Foothold Dynamic Feasibility Evaluation

We evaluate the dynamic transition feasibility on a stair climbing scenario. We compute a set of nominal future foothold locations assuming a periodic gait during one gait cycle (as described in [16]) and then we correct them with the VFA [9]. Subsequently, we check if there exists a trajectory that solves the problem formulated in (4a) for every candidate foothold. If the solution exists, the foothold is deemed dynamically feasible. Additionally we compute a cost map to visualize the “quality” of the solution provided by each candidate foothold. Fig. 4 shows an example of evaluated candidate footholds for the RF leg during a crawl while climbing stairs. Each pixel in the figure represents a candidate landing location. The importance of the Dynamic Optimizer is evident since some footholds deemed feasible using the VFA (Fig. 4 on the left) are discarded since no feasible trajectories to solve (4a) was found.

#### C. Experiments

Section V-C of [1] shows and discusses simulation results, while in this section we evaluate the hardware feasibility of the optimized trajectories on the quadruped

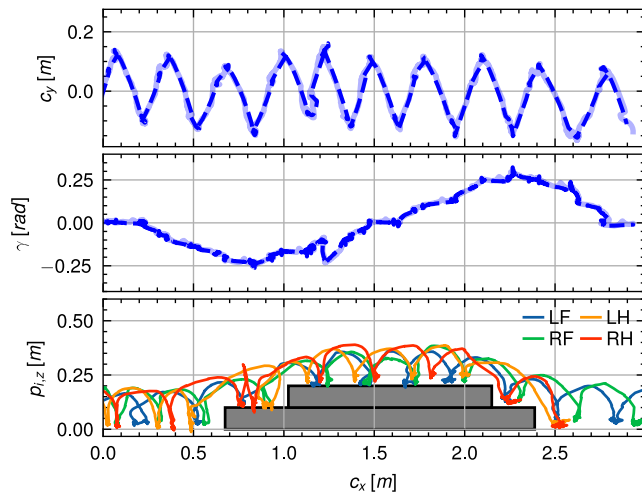


**Fig. 5:** Stairs experiment with nonlinear approach. For the top two plots, dashed lines are reference and solid lines are tracking signal. The top plot shows the CoM trajectory tracking on the  $xy$  plane and the middle plot shows the pitch tracking. On the last row we show the feet trajectories, where LF:Left Front, RF:Right Front, LH:Left Hind, and RH:Right Hind.

robot hydraulically actuated quadruped robot HyQ [17]. We decided to test the trajectory generated by the nonlinear formulation since it is the one that proved better in terms of generated trajectories. The scenario tested is shown in the snapshots of Fig. 1. It consists of climbing and descending two steps of 8cm each. Fig. 5 shows the tracking of the CoM trajectory on the  $xy$  plane and the pitch of the robot. As it can be seen, the robot is able to cross the scenario with a low tracking error in both position and orientation

#### IV. CONCLUSIONS

We presented a foothold evaluation criterion to assess the existence of dynamically feasible trajectories for legged locomotion that considers both linear and angular dynamics [1]. We extended the method in [2] by formulating the problem allowing variations in the angular momentum along the trajectory (i.e.,  $\dot{\mathbf{L}} \neq 0$ ) as a function of a desired angular trajectory. We presented two different formulations (a convex and a nonlinear) both able to generate feasible CoM trajectories.

As future work we aim to extend the proposed formulations to include more dynamic gaits, such as trot, and to design a learning algorithm that is able to approximate the proposed formulations, reducing computational burden.

#### REFERENCES

- [1] L. Clemente, O. Villarreal, A. Bratta, M. Focchi, V. Barasuol, G. Muscolo, and C. Semini, "Foothold evaluation criterion for dynamic transition feasibility for quadruped robots," in *IEEE International Conference on Robotics and Automation (ICRA)*, 2022.
- [2] P. Fernbach, S. Tonneau, O. Stasse, J. Carpentier, and M. Taïx, "C-croc: Continuous and convex resolution of centroidal dynamic trajectories for legged robots in multicontact scenarios," *IEEE Transactions on Robotics*, vol. 36, no. 3, pp. 676–691, 2020.
- [3] A. W. Winkler, C. D. Bellicoso, M. Hutter, and J. Buchli, "Gait and trajectory optimization for legged systems through phase-based end-effector parameterization," *IEEE Robotics and Automation Letters*, vol. 3, no. 3, pp. 1560–1567, July 2018. [Online]. Available: <https://doi.org/10.1109/LRA.2018.2798285>

- [4] M. Neunert, F. Farshidian, A. W. Winkler, and J. Buchli, "Trajectory Optimization Through Contacts and Automatic Gait Discovery for Quadrupeds," *IEEE Robotics and Automation Letters*, vol. 2, no. 3, pp. 1502–1509, 2017.
- [5] B. Aceituno-Cabezas, C. Mastalli, H. Dai, M. Focchi, A. Radulescu, D. G. Caldwell, J. Cappellotto, J. C. Grieco, G. Fernández-López, and C. Semini, "Simultaneous contact, gait, and motion planning for robust multilegged locomotion via mixed-integer convex optimization," *IEEE Robotics and Automation Letters*, vol. 3, no. 3, pp. 2531–2538, July 2018. [Online]. Available: <https://doi.org/10.1109/LRA.2017.2779821>
- [6] D. Orin, A. Goswami, and S.-H. Lee, "Centroidal Dynamics of a Humanoid Robot," *Autonomous Robots*, vol. 35, 10 2013.
- [7] M. Kalakrishnan, J. Buchli, P. Pastor, and S. Schaal, "Learning locomotion over rough terrain using terrain templates," in *2009 IEEE/RSJ International Conference on Intelligent Robots and Systems*, 2009, pp. 167–172.
- [8] O. Villarreal, V. Barasuol, P. M. Wensing, D. G. Caldwell, and C. Semini, "Mpc-based controller with terrain insight for dynamic legged locomotion," in *2020 IEEE International Conference on Robotics and Automation (ICRA)*, 2020, pp. 2436–2442.
- [9] O. Villarreal, V. Barasuol, M. Camurri, L. Franceschi, M. Focchi, M. Pontil, D. G. Caldwell, and C. Semini, "Fast and continuous foothold adaptation for dynamic locomotion through cnns," *IEEE Robotics and Automation Letters*, pp. 1–1, 2019.
- [10] D. Esteban, O. Villarreal, S. Fahmi, C. Semini, and V. Barasuol, "On the Influence of Body Velocity in Foothold Adaptation for Dynamic Legged Locomotion via CNNs," in *International Conference on Climbing and Walking Robots (CLAWAR)*, Moscow, Russia, Aug. 2020, pp. 353–360.
- [11] V. Barasuol, M. Camurri, S. Bazeille, D. G. Caldwell, and C. Semini, "Reactive trotting with foot placement corrections through visual pattern classification," in *2015 IEEE/RSJ International Conference on Intelligent Robots and Systems (IROS)*, September 2015, pp. 5734–5741. [Online]. Available: <https://doi.org/10.1109/IROS.2015.7354191>
- [12] D. Belter, J. Bednarek, H. Lin, G. Xin, and M. Mistry, "Single-shot Foothold Selection and Constraint Evaluation for Quadruped Locomotion," in *2019 International Conference on Robotics and Automation (ICRA)*, 2019, pp. 7441–7447.
- [13] L. Chen, S. Ye, C. Sun, A. Zhang, G. Deng, T. Liao, and J. Sun, "CNNs based Foothold Selection for Energy-Efficient Quadruped Locomotion over Rough Terrains," in *2019 IEEE International Conference on Robotics and Biomimetics (ROBIO)*, 2019, pp. 1115–1120.
- [14] P. Fankhauser, M. Bjelonic, C. Dario Bellicoso, T. Miki, and M. Hutter, "Robust Rough-Terrain Locomotion with a Quadrupedal Robot," in *2018 IEEE International Conference on Robotics and Automation (ICRA)*, 2018, pp. 5761–5768.
- [15] F. Jenelten, T. Miki, A. E. Vijayan, M. Bjelonic, and M. Hutter, "Perceptive Locomotion in Rough Terrain – Online Foothold Optimization," *IEEE Robotics and Automation Letters*, vol. 5, no. 4, pp. 5370–5376, 2020.
- [16] N. Rathod, A. Bratta, M. Focchi, M. Zanon, O. Villarreal, C. Semini, and A. Bemporad, "Model predictive control with environment adaptation for legged locomotion," pp. 145 710–145 727, 2021.
- [17] C. Semini, N. G. Tsagarakis, E. Guglielmino, M. Focchi, F. Cannella, and D. G. Caldwell, "Design of hyq - a hydraulically and electrically actuated quadruped robot," *IMEchE Part I: Journal of Systems and Control Engineering*, vol. 225, no. 6, pp. 831–849, 2011.